JOC The Journal of Organic Chemistry

pubs.acs.org/joc Note

Synthesis of Biologically Active Heterospirocycles through Iterative 1,3-Dipolar Cycloaddition Pathways

Pallavi Sharma,* M. R. Ranga Prabhath, Derek Wong, Maame Adjoa Ampem-Lassen, Shreesha V. Bhat, Luke Williams, and Teresa G. Carvalho

Cite This: https://dx.doi.org/10.1021/acs.joc.0c02424 Read Online

ACCESS | Metrics & More | Article Recommendations | Supporting Information

ABSTRACT: We demonstrate the novel spiroannulation of *exo*-imines with 1,3-dipoles, for the first time, leading to 3D spirocycles with a secondary amine (NH) in the spiro-ring. The synthetic method described herein allows access to these previously unexplored heterospirocyclic cores that have application in the discovery of functional molecules for medicinal and materials science. This was demonstrated by discovering an unprecedented class of heterospirocycles with antimalarial activity against the human protozoan *P. falciparum*.

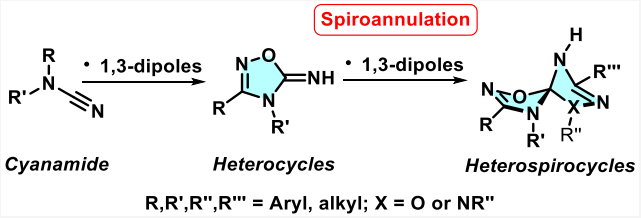

The three-dimensional (3D) spirane scaffold, comprising both fused rings and quaternary stereocenter (sp^3), offers a foundation for building molecular complexity and diversity about a compact core, playing an essential role in the search for function.[1−4] Spiranes are integral components of many biologically active natural products (e.g., griseofulvin, Scheme 1A)[5,6] and appear in clinically used drugs (e.g., irbesartan, Scheme 1A).[7,8] The exit vectors of the 3D molecules facilitate a significantly greater interaction of the ligand with the 3D binding site of the biological targets inaccessible to a flat (hetero)aromatic ring.[9] Furthermore, the restricted maneuverability within the conformationally rigid spirocycles reduces the number of possible conformations (distinct 3D shapes) that a molecule can adopt, which may lead to higher potency and selectivity.[9,10]

Spirocycles are considered synthetically challenging targets, not least due to the quaternary stereocenter.[11] Both inter- and intramolecular strategies, such as (i) intramolecular substitution of a halogen or activated alcohol, (ii) intermolecular ring synthesis from doubly activated substrates, (iii) radical cyclization, and (iv) cycloaddition reactions, are the most commonly employed key steps.[3,11] Ring combination statistics studies of biologically relevant spirocycles reveal that the number of distinct multiheteroatom-containing rings, on average, are less prevalent compared to carbon-rich spirocycles. The ring combinations of five-membered [4.4], six-membered [5.5], and five- and six-membered [4.5] rings are also more common.[1] Hence, to maintain the momentum and the diversity in the drug discovery supply chain, technological advances that provide routes to multiheteroatom-containing spirocycles are warranted.

Huisgen-type 1,3-dipolar cycloaddition reactions are practical transformations for the rapid generation of molecular complexity by building new heteroatom-rich ring systems with stereocenters.[12,13] The 1,3-dipolar cycloaddition approach to access spirocycles involves either the (i) construction of a new ring on an existing carbo- or heterocycle[14,15] or (ii) simultaneous formation of two rings through a double 1,3-dipolar cycloaddition of a diene such as allenoates.[16,17]

Huisgen and co-workers demonstrated seminal examples of carbodiimides[18] and cyanamides[19−21] as useful "templates" for generating nitrogen-rich ring systems including spirocycles. In a rare example of a spirocycle synthesis via a double 1,3-dipolar cycloaddition reaction for heterospirocycle synthesis, Huisgen et al. reported the spiroannulation of carbodiimides (**7**) with hydrazonyl chloride (**1**), giving the all-substituted hexaazospiranes such as **8** (5 examples, Scheme 1B). This report is the only example of nitrogen-rich spirocycles of this class.[18] The related approach to access the spirocycle such as **3**, through the one-pot reaction of phenyl cyanamide (**2**) (1 equiv) with **1** (2 equiv) via an intermediate 1,2,4 triazol-*exo*-imine (**6**), proved unsuccessful.[19,20] As spirocycle **3** was not detected or isolated, the authors suggest "such compounds are not stable if they have NH groups"[22] and, instead, led to the formation of two isomeric products, **4** and **5**, via ring-opening of 4−5 and 1′−5 bonds, respectively, of the spiro **3** (Scheme 1B).[19]

We have reported a method for the generation and capture of cyanamide anions[21] with 1,3-dipoles to give five-membered heterocyclic rings.[23,24] Through a formal 1,3-dipolar cyclo-

Received: October 13, 2020

https://dx.doi.org/10.1021/acs.joc.0c02424
J. Org. Chem. XXXX, XXX, XXX−XXX

Scheme 1. (A) Spirocycle Containing Natural Products and Drug Leads; (B) Huisgen's Seminal Work on the Use of Cyanamide and Carbodiimide in the Spirocyclization Reaction; (C) New Method for the Synthesis of the Heterospirocycle via Iterative 1,3-Dipolar Cycloadditions with Cyanamide

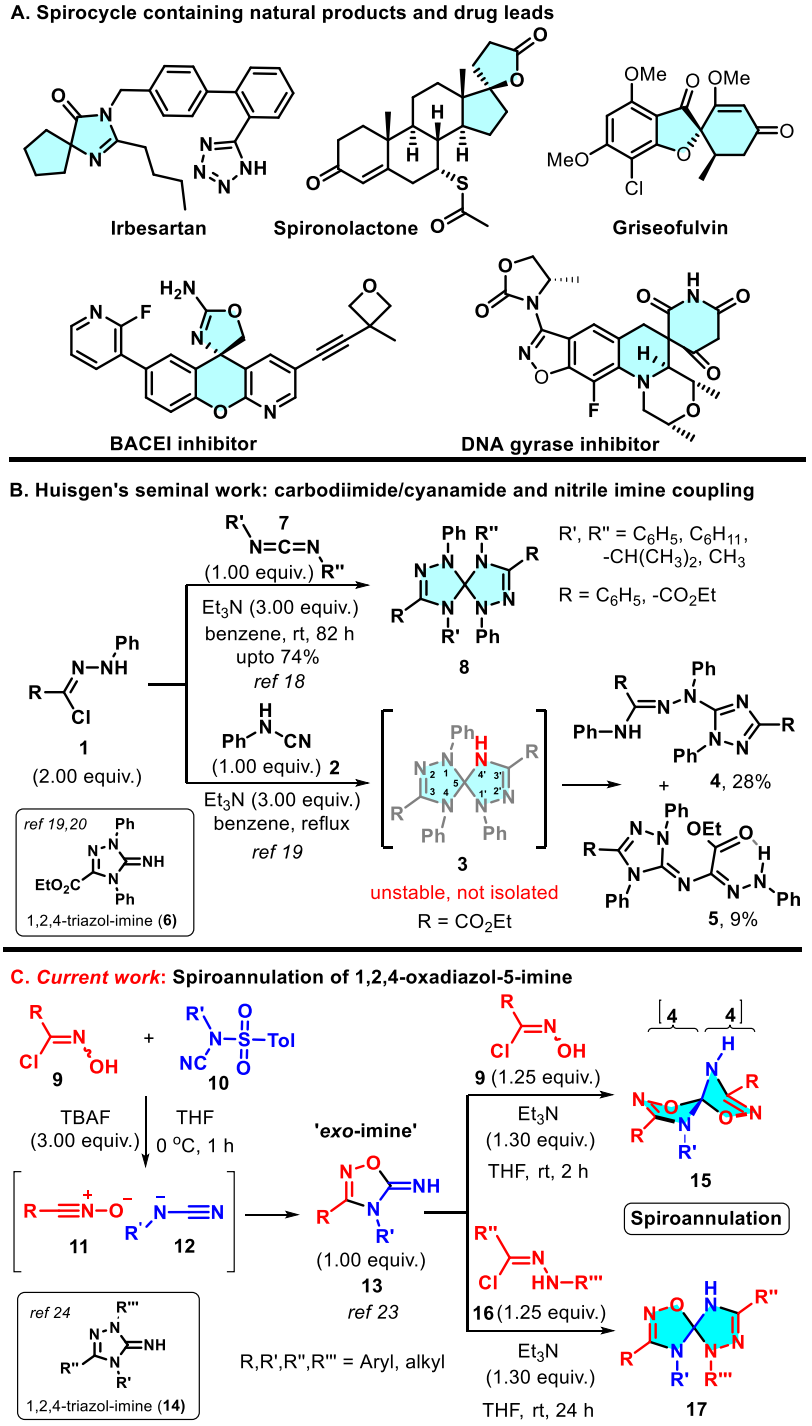

addition strategy, the amine nitrogen of the cyanamide ion (**12**) was incorporated in the ring's core to give *exo*-imine structures such as oxadiazol-imine[23] **13** and triazol-imine[24] **14** (Scheme 1C). These rare heterocyclic cores not only function as novel pharmacophores,[25] but the newly formed *exo*-imines are themselves primed to offer new structures such as oxadiazolone after hydrolysis and amidine upon further decarboxylation.[23,24]

These *exo*-imine dipolarophiles lend themselves to spiroannulation reactions with appropriate dipolar partners to create new rings via two new bonds.[26] For example, a second [3+2] 1,3-dipolar cycloaddition of a nitrile oxide or nitrile imine dipole with **13** would deliver structures like **15** and **17**, in which case two five-membered rings ([4.4] spiro)[27] are bound through a single C atom (Scheme 1C).

Revisiting the reaction pathways proposed by Huisgen to access spirocyclic structures containing NH functionality, we herein report the first general example of siproannulation of *exo*-imines leading to the isolation and characterization of nitrogen-rich spirocyclic scaffolds with NH functionality. Our

https://dx.doi.org/10.1021/acs.joc.0c02424
J. Org. Chem. XXXX, XXX, XXX−XXX

approach enables the synthesis of various fused ring systems, such as spirobisoxadiazoline (**15**) and spiro-oxadiazoline-triazoline (**17**), depending on the dipoles employed.

For our initial studies, we chose the oxadiazol-imine **18** (1.00 equiv),[23] and the nitrile oxide precursor, chloroxime **19**, (1.25 equiv) as model substrates, combined with excess triethylamine (Et_3N) (6.4 equiv). Both the nitrile oxides and nitrile imines 1,3-dipoles are versatile reactive partners and are routinely generated *in situ* under mild conditions through the base or fluoride ion activation.[28−30] These dipoles, however, have a short half-life and are prone to self-dimerization.[30−35] Upon stirring at room temperature (rt) for 24 h in tetrahydrofuran (THF), the spirocycle **20** was isolated in 59% yield. The atom connectivity of **20** was established following multiple analytical experiments (see Supporting Information) and corroborated through single-crystal X-ray diffraction (see Supporting Information).[36]

During our preliminary investigation, the well-established homocoupled nitrile oxide dimer **21** was detected as a side product (12%).[23,28,30,31] Therefore, optimization studies were performed to find conditions that circumvent dimer **21** formation, thereby improving the yield of **20**.

The screening of different bases and fluoride ion sources for nitrile oxide generation, the order and rate of the addition of the substrates and reagents, reaction times, and solvents (see Supporting Information), revealed the optimal conditions: treating a mixture of **18** (1.00 equiv) and **19** (1.25 equiv) in THF with the slow addition of Et_3N (1.30 equiv) over 2 h at rt (Table 1, entry 8). Comparative yields could also be achieved when CsF/18-crown-6 is used as the fluoride ion source for dehydrochlorination of **19** (Table 1, entry 4).[35]

Table 1. Optimization Study for the Spirocyclization Reaction

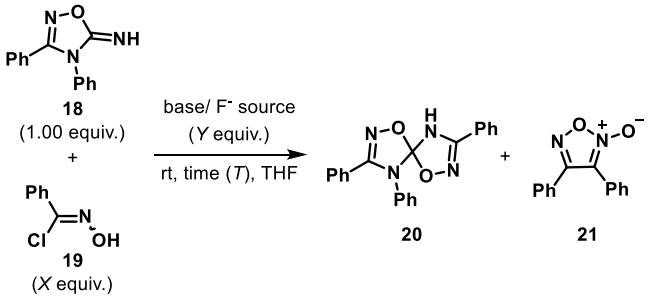

entry[a,b]	**19** (equiv)	base/F^- (equiv)	time (h)	yield (%)[c]
1	1.25	Et_3N[d] (6.4)	24	59
2	1.25	Et_3N[d] (1.3)	24	81
3	1.25	TBAF[d] (1.3)	24	*e*
4[f]	1.25	CsF/18C[g] (1.3)	24	75
5	1.25	DIPEA[d] (1.3)	24	68
6[f]	1.25	K_2CO_3[h] (1.3)	24	*e*
7	2	Et_3N[d] (1.3)	10	81
8	1.25	Et_3N[d] (1.3)	2	77
9	1.25		48	56

[a]Reactions were performed on a 0.1 mmol scale with respect to **18**. [b]0.22 M solution with respect to **18**. [c]Isolated yield. [d]Addition over 2 h using a syringe pump. [e]No reaction as indicated by NMR analysis of the crude reaction mixture. [f]The base/F^- was first introduced to **18** followed by the addition of **19** over 2 h. [g]CsF:18-C-6 (1:1). [h]Added in one portion.

Using these new, improved conditions, we synthesized a focused library of structurally novel nitrogen-rich spirocycles. Various oxadiazol-imine cores with substitution on the A ring (**18′**, Scheme 2) underwent smooth ring annulation with

Scheme 2. Synthesis of 1,6-Dioxa-2,4,7,9-tetraazaspiro[4.4]nona-2,7-dienes[a]

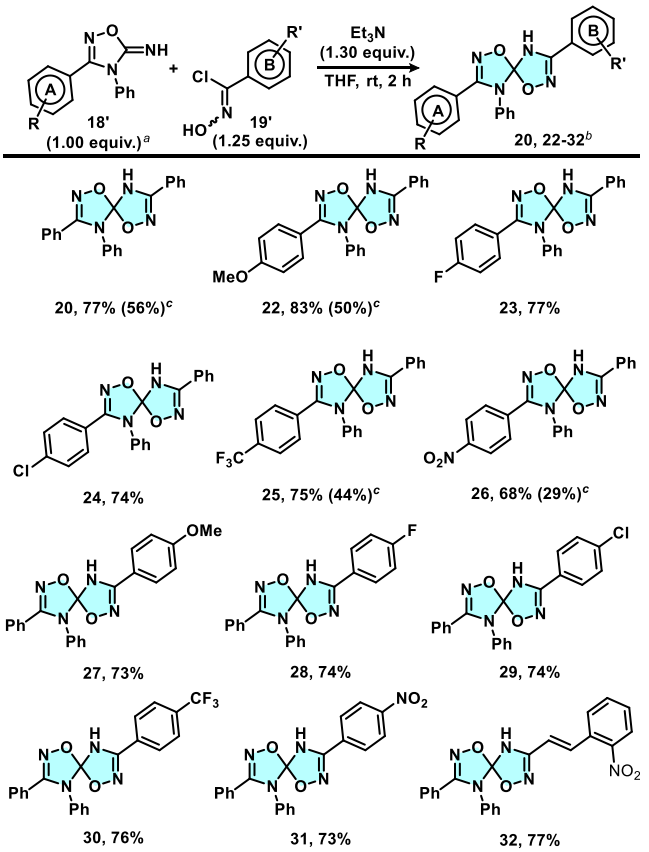

[a]Reactions were performed on a 0.22 mmol scale with respect to **18′**. [b]Isolated yield. [c]No additives.

nitrile oxides to offer the spirocyclic products **20** and **22**−**32** in good to excellent yields.[37] The electron-donating (—OCH_3) substituent on the A ring gave the highest yield of 83% (product **22**). The yield gradually decreased with the increase in the electron-withdrawing nature of the substituent on the A ring (**24**−**26**). On the other hand, no significant effect on yield was noted upon varying the substituents' donor−acceptor properties attached to the chloroxime substrates (B ring, **19′**, Scheme 2) (**27**−**31**). This observation suggests that the nucleophilicity of the oxadiazol-*exo*-imine nitrogen (=NH) plays a significant role in driving the spirocyclization reaction forward.

Though Et_3N was employed as the base to generate the reactive dipoles from the corresponding chloroximes for optimum product yields, the reaction was found to deliver the spirocyclic product in the absence of any externally added base or fluoride ion, indicating a self-catalyzed reaction (Table 1, entry 9). It is plausible that the *exo*-imines could itself act as a base to assist the removal of HCl from the chloroximes to offer the reactive nitrile oxide intermediates; alternatively, the *exo*-imines may participate in a tandem nucleophilic addition−elimination reaction with chloroximes to offer the final spirocyclized products (see Supporting Information).[38] How-

https://dx.doi.org/10.1021/acs.joc.0c02424
J. Org. Chem. XXXX, XXX, XXX−XXX

ever, the reaction was found to be sluggish, providing products only in a low to moderate yield (29−56%, **20**, **22**, **25**, **26**, Scheme 2).

On the contrary, the cycloaddition reaction between **18** and **19** was completely suppressed when an additive such as TBAF or K_2CO_3 was employed for the *in situ* generation of nitrile oxide[23,28,30] (Table 1, entries 3 and 6). This also explains the failure to access spirocycles under a "one-pot, two-step" protocol via iterative dipolar cycloaddition reactions between cyanamide (**10**) and chloroxime (**9**) without isolating the intermediate *exo*-imine dipolarophile (**13**)[23] in the presence of TBAF (see Supporting Information).

Continuing with our theme to showcase the *exo*-imine substrates' versatility for complexity generation, we next explored the synthesis of sterically congested oxa-pentaazaspiranes (**17**, Scheme 1), employing nitrile imine dipoles. Like the nitrile oxides, nitrile imine dipoles are reactive, short-lived, and challenging species to engage in intermolecular cycloaddition reactions with complementary reactive partners.[24,29] Gratifyingly, several bis-aryl-substituted oxa-pentaazaspiranes (**33**−**37**) were readily obtained under standardized reaction conditions, albeit with an extended reaction time of 24 h (Scheme 3). The successful isolation of a range of dioxa-

Scheme 3. Synthesis of 1-Oxa-2,4,6,7,9-pentaazaspiro[4.4]nona-2,7-diene[a]

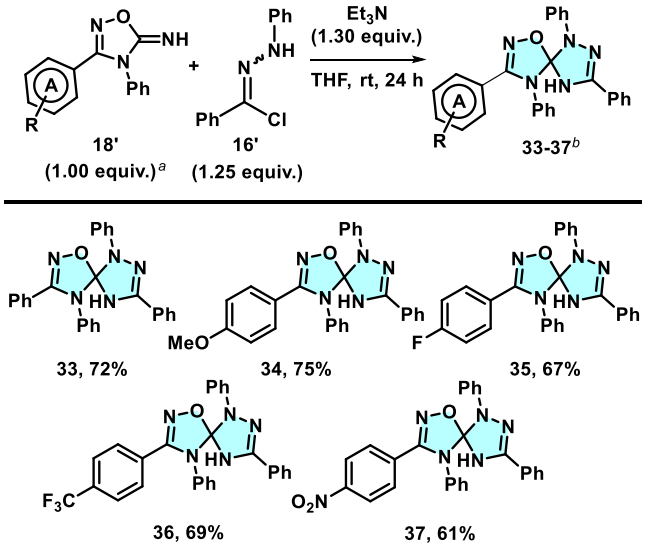

[a]Reactions performed on a 0.22 mmol scale with respect to **18′**. [b]Isolated yield.

tetraazaspiranes (**20**, **22**−**32**) and oxa-pentaazaspiranes (**33**−**37**) demonstrates their stability when compared to the Huisgen-type spiro **3**.[19]

Spirocyclic drugs have been known for over 50 years and have been used to target various drug targets. These includes the aspartyl protease, BACE1, as a therapeutic for Alzheimer's disease;[39] and as a DNA gyrase inhibitor, which has entered clinical trials for the treatment of gonorrhea.[40] Hence, to fully exploit the potential of our in-house synthesized library of novel and diverse spirocyclic scaffolds, we elected to screen against human protozoa.

The antimicrobial properties of the compounds **20**, **22**−**31**, and **33**−**37** were tested against *Plasmodium falciparum*, the most virulent of human malaria parasites.[41] The *in vitro* drug screen assays determined that four compounds (**25**, **26**, **36**, and **37**) have an antiplasmodial activity with IC_{50} values in the low micromolar range (Figure 1 and Supporting Information). Furthermore, a significant decrease in parasite load and death phenotypes was observed within the first 24 h post drug incubation at 10 μM concentration. Two gold standard antimalarial drugs, artemisinin[42] and chloroquine,[43] was included in our assays as positive controls for parasite death and comparison of drug efficacy. Although the spirocycles displayed lower efficacy than artemisinin, their unprecedented structures represent a new class of nitrogen-rich spirocyclic compounds to the malarial community. Drug-resistant malaria has emerged against all available treatments,[43] and new classes of antimalarials have not been introduced into clinical practice since 1996.[44] The two spirocycles, **25** and **26**, therefore, are promising leads for antimalarial drugs developments.

In summary, we have shown the incorporation of the N−C−N connectivity of cyanamides into novel spirocyclic pharmacophores via an iterative cycloaddition strategy. The novel spiranes containing a secondary cyclic amine (NH) were isolated and characterized for the first time. Furthermore, our new chemistry delivered an unprecedented class of nitrogen-rich 3D heterospirocycle as antimalarial agents with activity against the human protozoan *P. falciparum*. The target of these spirocycle compounds is yet to be identified and is currently under investigation.

EXPERIMENTAL SECTION

General Consideration. ^{1}H NMR and ^{13}C NMR spectra were recorded on a (i) Bruker AV 500 spectrometer at 500 and 125 MHz, respectively, and a (ii) Bruker Ascend 400 (400 MHz) at 400 and 100 MHz, respectively. High-resolution mass spectra (HRMS) were obtained at the National Mass Spectrometry Facility in Swansea, UK, or on a VG micron Autospec or Bruker microTOF or using an Agilent 6530 accurate-mass Q-TOF LC/MS in electrospray ionization (ESI). Infrared spectra were obtained on a PerkinElmer Spectrum 100 FT-IR Universal ATR Sampling Accessory or Bruker Alpha FT-IR spectrometer, deposited neat to a diamond/ZnSe plate. The melting point was recorded on a Stuart SMP10 digital or Gallenkamp melting point apparatus. Single-crystal X-ray crystallography was recorded on Bruker D8 Venture with Ius 3.0 Cu and Ius 3.0 Mo.

Column chromatography was carried out using silica gel 60, and thin-layer chromatography was performed using silica gel 60 F254 precoated sheets and visualized by UV (254 nm). Hex refers to hexane, EA refers to ethyl acetate, and Et_3N refers to triethylamine. All chemicals were used without further purification unless otherwise stated. Dry THF refers to the commercially procured anhydrous solvent.

General Procedure for the Synthesis of Dioxa-tetraazaspiro Compounds (20, 22−32). In a 5 mL round-bottom flask, 1,2,4-oxadiazol-5(4*H*)-imine[23] (0.220 mmol, 1.00 equiv) and the respective hydroxymoyl chloride (1.25 equiv) were dissolved in a portion of dry THF (1.00 mL, 0.22 M), and the mixture was stirred for 5 min at room temperature. Triethyl amine (Et_3N) (1.30 equiv) was diluted in 0.50 mL of dry THF (0.57 M) and was introduced to the reaction mixture dropwise over 2 h. The completion of the reaction was monitored on TLC using the 5:2 Hex/EA mobile phase. Once the reaction has reached completion, the solvent was evaporated *in vacuo*, and the crude mixture was purified by column chromatography using a Hex/EA (5%−20%) mobile phase.

General Procedure for the Synthesis of Oxa-pentaazaspiro Compounds (33−37). In a 5 mL round-bottom flask, 1,2,4-oxadiazol-5(4*H*)-imine[23] (0.220 mmol, 1.00 equiv) and the respective hydrazonyl chloride (1.25 equiv) were dissolved in a portion of dry THF (1.00 mL, 0.22 M), and the mixture was stirred for 5 min at rt. Et_3N (1.3 equiv) was diluted in 0.50 mL of dry THF (0.57 M) and was introduced to the reaction mixture dropwise over 2 h. The

https://dx.doi.org/10.1021/acs.joc.0c02424
J. Org. Chem. XXXX, XXX, XXX−XXX

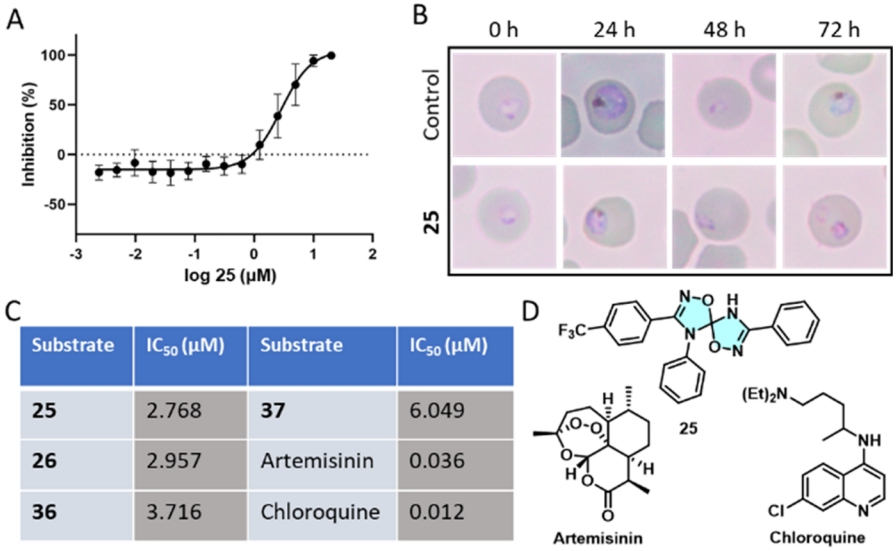

Substrate	IC_{50} (μM)	Substrate	IC_{50} (μM)
25	2.768	**37**	6.049
26	2.957	Artemisinin	0.036
36	3.716	Chloroquine	0.012

Figure 1. Drug screen against the human malaria parasite *Plasmodium falciparum*. (A) Growth inhibition assay of compound **25** (n = 6). (B) Phenotypic assay of *P. falciparum* in the presence of 10 μM compound **25**. After a 24 h compound incubation, *P. falciparum* parasites (trophozoite stage) present a significant growth defect when compared to the no drug control. Characteristic dead parasite forms are observed at 48 and 72 h post drug incubation, while the no drug condition produces ring and trophozoite stages, respectively. (C) IC_{50} values of compounds **25**, **26**, **36**, and **37** that impact *in vitro* parasite growth. (D) Structure comparison of **25** with leading antimalarial drugs.

resulting mixture was stirred for 24 h at rt. Completion of the reaction was monitored on TLC using the 5:2 Hex/EA mobile phase. Once completed, the solvent was evaporated *in vacuo*, and the crude mixture was purified by column chromatography using a Hex/EA (5%−20%) mobile phase.

Large-Scale Synthesis of 20. In a 50 mL round-bottom flask, 3,4-diphenyl-1,2,4-oxadiazol-5(4*H*)-imine (0.500 g, 2.10 mmol) and (*Z*)-*N*-hydroxybenzimidoyl chloride (0.410 g, 2.60 mmol, 1.25 equiv) were dissolved in 10 mL of dry THF, and the mixture was stirred for 5 min at room temperature. Triethyl amine (Et_3N) (2.73 mmol, 0.38 mL) was diluted in 5 mL of dry THF and was introduced to the reaction mixture dropwise over 2 h. The completion of the reaction was monitored on TLC using a 5:2 Hex/EA mobile phase. Once the reaction has reached completion, the solvent was evaporated *in vacuo*, and the crude mixture was purified by column chromatography using a Hex/EA (5%−20%) mobile phase to give **20** in 69% yield (0.520 g).

*3,4,8-Triphenyl-1,6-dioxa-2,4,7,9-tetraazaspiro[4.4]nona-2,7-diene (**20**).* Compound **20** was obtained in 77% yield (60 mg) as a white solid: R_f 0.59 (5:2 Hex/EA); mp 131−133 °C (decomposed); ^{1}H NMR ($(CD_3)_2CO$, 500 MHz) δ 11.40 (br s, 1H), 7.99 (d, J = 6.7 Hz, 2H), 7.84 (d, J = 5.7 Hz, 2H), 7.49−7.55 (m, 3H), 7.59 (d, J = 7.8 Hz, 2H), 7.38−7.46 (m, 5H), 7.24−7.27 (m, 1H); $^{13}C\{^1H\}$ NMR ($(CD_3)_2CO$, 125 MHz) δ 170.3, 169.3, 146.6, 139.9, 132.5, 132.0, 131.2, 130.3, 129.8, 129.7, 128.5, 127.9, 127.8, 127.2, 124.1; IR ν (cm^{-1}) 3170 (broad), 1568, 1492, 1402, 1238; HRMS (ASAP+) m/z $[M + H]^+$ calcd for $C_{21}H_{16}N_4O_2H$ 357.1352, found 357.1343.

*3-(4-Methoxyphenyl)-4,8-diphenyl-1,6-dioxa-2,4,7,9-tetraazaspiro[4.4]nona-2,7-diene (**22**).* Compound **22** was obtained in 83% yield (71 mg) as a white solid: R_f 0.50 (5:2 Hex/EA); mp 98−100 °C (decomposed); ^{1}H NMR ($(CD_3)_2CO$, 500 MHz) δ 7.99 (d, J = 6.7 Hz, 2H), 7.76 (d, J = 8.8 Hz, 2H), 7.59 (d, J = 7.8 Hz, 2H), 7.48−7.54 (m, 3H), 7.43 (t, J = 7.9 Hz, 2H), 7.23−7.27 (m, 1H), 6.94 (d, J = 8.8 Hz, 2H), 3.79 (s, 3H); $^{13}C\{^1H\}$ NMR ($(CD_3)_2CO$, 100 MHz) δ 170.3, 169.3, 162.4, 146.4, 140.0, 131.9, 130.2, 129.7, 129.3, 128.5, 127.9, 127.1, 124.7, 124.0, 115.1, 55.8; IR ν (cm^{-1}) 1566, 1500, 1386, 1262; HRMS (ASAP+) m/z $[M + H]^+$ calcd for $C_{22}H_{18}N_4O_3H$ 387.1457, found 387.1451.

*3-(4-Fluorophenyl)-4,8-diphenyl-1,6-dioxa-2,4,7,9-tetraazaspiro-[4.4]nona-2,7-diene (**23**).* Compound **23** was obtained in 77% yield (63 mg) as a white solid: R_f 0.59 (5:2 Hex/EA); mp 142−144 °C (decomposed); ^{1}H NMR ($(CD_3)_2CO$, 500 MHz) δ 11.43 (br s, 1H), 7.98 (d, J = 6.7 Hz, 2H), 7.87−7.92 (m, 2H), 7.59 (d, J = 7.6 Hz, 2H), 7.49−7.55 (m, 3H), 7.44 (t, J = 7.9 Hz, 2H), 7.25−7.29 (m, 1H), 7.17 (t, J = 8.8 Hz, 2 H); $^{13}C\{^1H\}$ NMR ($(CD_3)_2CO$, 125 MHz) δ 170.2, 169.5, 164.8 (J = 248.8 Hz), 145.8, 139.7, 132.0, 130.3, 130.1 (J = 8.1 Hz), 129.8, 128.5, 127.9, 127.3, 124.2, 116.7 (J = 22.7 Hz); IR ν (cm^{-1}) 3164 (broad), 1514, 1436, 1228; HRMS (ASAP+) m/z $[M + H]^+$ calcd for $C_{21}H_{15}N_4O_2FH$ 375.1257, found 375.1248.

*3-(4-Chlorophenyl)-4,8-diphenyl-1,6-dioxa-2,4,7,9-tetraazaspiro[4.4]nona-2,7-diene (**24**).* Compound **24** was obtained in 74% yield (64 mg) as a white solid: R_f 0.63 (5:2 Hex/EA); mp 146−148 °C (decomposed); ^{1}H NMR ($(CD_3)_2CO$, 500 MHz) δ 11.55 (br s, 1H), 7.98 (d, J = 6.8 Hz, 2H), 7.86 (d, J = 8.5 Hz, 2H), 7.58 (d, J = 7.6 Hz, 2H), 7.49−7.55 (m, 3H), 7.42−7.46 (m, 4 H), 7.25−7.29 (m, 1H); $^{13}C\{^1H\}$ NMR ($(CD_3)_2CO$, 125 MHz) δ 170.2, 169.3, 145.8, 139.7, 136.6, 132.0, 131.4, 130.4, 129.9, 129.8, 129.4, 128.4, 127.9, 127.4, 124.1; IR ν (cm^{-1}) 1566, 1500, 1386, 1262; IR ν (cm^{-1}) 1510, 1434, 1218; HRMS (ASAP+) m/z $[M + H]^+$ calcd for $C_{21}H_{15}N_4O_2ClH$ 391.0962, found 391.0954.

*4,8-Diphenyl-3-(4-(trifluoromethyl)phenyl)-1,6-dioxa-2,4,7,9-tetraazaspiro[4.4]nona-2,7-diene (**25**).* Compound **25** was obtained in 75% yield (70 mg) as a white solid: R_f 0.65 (5:2 Hex/EA); mp 96−97 °C (decomposed); ^{1}H NMR ($(CD_3)_2CO$, 500 MHz) δ 11.79 (br s, 1H), 8.08 (d, J = 7.9 Hz, 2H), 7.98 (d, J = 6.9 Hz, 2H), 7.76 (d, J = 8.2 Hz, 2H), 7.61 (d, J = 7.6 Hz, 2H), 7.49−7.55 (m, 3H), 7.45 (t, J = 7.8 Hz, 2H), 7.26−7.30 (m, 1H); $^{13}C\{^1H\}$ NMR ($(CD_3)_2CO$, 125 MHz) δ 170.1, 169.4, 145.7, 139.6, 136.6, 132.3, 132.1, 131.9, 130.5, 129.8, 128.5, 128.4, 127.9, 127.5, 126.7−126.8 (q, J = 4.5 Hz), 124.2; IR ν (cm^{-1}) 1498, 1390, 1318, 1118; HRMS (ASAP+) m/z $[M + H]^+$ calcd for $C_{22}H_{15}N_4O_2F_3H$ 425.1225, found 425.1215.

*3-(4-Nitrophenyl)-4,8-diphenyl-1,6-dioxa-2,4,7,9-tetraazaspiro-[4.4]nona-2,7-diene (**26**).* Compound **26** was obtained in 68% yield (60 mg) light yellow solid: R_f 0.42 (5:2 Hex/EA); mp 164−166 °C (decomposed); ^{1}H NMR ($(CD_3)_2CO$, 500 MHz) δ 11.95 (br s, 1H), 8.26 (d, J = 8.5 Hz, 2H), 8.13 (d, J = 8.6 Hz, 2H), 7.98 (d, J = 6.9 Hz, 2H), 7.61 (d, J = 7.8 Hz, 2H), 7.44−7.55 (m, 5H), 7.27−7.32 (m, 1H); $^{13}C\{^1H\}$ NMR ($(CD_3)_2CO$, 125 MHz) δ 170.0, 169.4, 149.8, 145. 5, 139.4, 138.7, 132.1, 130.5, 129.8, 128.9, 128.3, 127.9, 127.7, 124. 9, 124.2; IR ν (cm^{-1}) 1568, 1502, 1400, 1350,1022; HRMS (NSI +) m/z $[M + H]^+$ calcd for $C_{21}H_{15}N_5O_4H$ 402.1197, found 402.1194.

*8-(4-Methoxyphenyl)-3,4-diphenyl-1,6-dioxa-2,4,7,9-tetraazaspiro[4.4]nona-2,7-diene (**27**).* Compound **27** was obtained in 73% yield (67 mg) as a white solid: R_f 0.55 (5:2 Hex/EA); mp

https://dx.doi.org/10.1021/acs.joc.0c02424
J. Org. Chem. XXXX, XXX, XXX−XXX

150−151 °C (decomposed); ^{1}H NMR ($(CD_3)_2CO$, 500 MHz) δ 11.38 (br s, 1H), 7.92 (d, J = 8.8 Hz, 2H), 7.80−7.86 (m, 2H), 7.58 (d, J = 7.8 Hz, 2H), 7.37−7.45 (m, 6H), 7.23−7.26 (m, 1H), 7.05 (d, J = 8.8 Hz, 2H), 3.86 (s, 3H); $^{13}C\{^1H\}$ NMR ($(CD_3)_2CO$, 125 MHz) δ 169.9, 169.1, 163.0, 146.7, 139.9, 132.6, 131.1, 130.3, 129.7, 129.6, 127.8, 127.1, 124.0, 120.8, 115.1, 55.9; IR ν (cm^{-1}) 1490, 1464, 1386, 1240; HRMS (NSI+) m/z $[M + H]^+$ calcd for $C_{22}H_{18}N_4O_3H$ 387.1457, found 387.1450.

*8-(4-Fluorophenyl)-3,4-diphenyl-1,6-dioxa-2,4,7,9-tetraazaspiro-[4.4]nona-2,7-diene (**28**).* Compound **28** was obtained in 74% yield (65 mg) as a white solid: R_f 0.69 (5:2 Hex/EA); mp 110−111 °C (decomposed); ^{1}H NMR ($(CD_3)_2CO$, 500 MHz) δ 11.48 (br s, 1H), 8.03 (br s, 2H), 7.83 (br. s., 2H), 7.56−7.63 (m, 2H), 7.38−7.45 (m, 5H), 7.27 (d, J = 8.4 Hz, 3H); $^{13}C\{^1H\}$ NMR ($(CD_3)_2CO$, 125 MHz) δ 170.3, 168.5, 165.3 (J = 248.8 Hz), 146.6, 139.8, 132.5, 131.1, 130.35 (J = 9.1 Hz), 130.2, 129.7, 127.8, 127.3, 124.1, 116.79 (J = 22.7 Hz); IR ν (cm^{-1}) 1568, 1496, 1386, 1230; HRMS (NSI+) m/z $[M + H]^+$ calcd for $C_{21}H_{15}N_4O_2FH$ 375.1252, found 375.1244.

*8-(4-Chlorophenyl)-3,4-diphenyl-1,6-dioxa-2,4,7,9-tetraazaspiro[4.4]nona-2,7-diene (**29**).* Compound **29** was obtained in 74% yield (68 mg) as a white solid: R_f 0.50 (5:2 Hex/EA); mp 101−102 °C (decomposed); ^{1}H NMR ($(CD_3)_2CO$, 500 MHz) δ 11.50 (br s, 1H), 7.99 (d, J = 8.1 Hz, 2H), 7.81−7.88 (m, 2H), 7.53−7.61 (m, 4 H), 7.38−7.45 (m, 5H), 7.23−7.28 (m, 1H); $^{13}C\{^1H\}$ NMR ($(CD_3)_2CO$, 125 MHz) δ 170.4, 168.5, 146.5, 139.8, 137.5, 132.4, 131.1, 130.3, 129.9, 129.7, 129.6, 129.6, 127.7, 127.3, 127.2, 124.1; IR ν (cm^{-1}) 1490, 1386, 1292; HRMS (NSI+) m/z $[M + H]^+$ calcd for $C_{21}H_{15}N_4O_2ClH$ 391.0956, found 391.0950.

*3,4-Diphenyl-8-(4-(trifluoromethyl)phenyl)-1,6-dioxa-2,4,7,9-tetraazaspiro[4.4]nona-2,7-diene (**30**).* Compound **30** was obtained in 76% yield (76 mg) as a white solid: R_f 0.67 (5:2 Hex/EA); mp 78−80 °C (decomposed); ^{1}H NMR ($(CD_3)_2CO$, 500 MHz) δ 8.20 (d, J = 7.93 Hz, 2H), 7.83−7.90 (m, 4 H), 7.61 (d, J = 7.63 Hz, 2H), 7.39−7.46 (m, 6H), 7.25−7.29 (m, 1H); $^{13}C\{^1H\}$ NMR ($(CD_3)_2CO$, 125 MHz) δ 170.7, 168.4, 146.5, 139.7, 132.4, 131.2, 130.5, 130.3, 129.8, 129.4, 128.7, 128. 6, 127. 8, 127.4, 126.7−126.8 (q, J = 3.6 Hz), 124.2; IR ν (cm^{-1}) 1500, 1394, 1320, 1112; HRMS (ESI+) m/z $[M + H]^+$ calcd for $C_{22}H_{15}N_4O_2F_3H$ 425.1220, found 425.1218.

*8-(4-Nitrophenyl)-3,4-diphenyl-1,6-dioxa-2,4,7,9-tetraazaspiro-[4.4]nona-2,7-diene (**31**).* Compound **31** was obtained in 73% yield (69 mg) as a light-yellow solid: R_f 0.65 (5:2 Hex/EA); mp 142−145 °C (decomposed); ^{1}H NMR ($(CD_3)_2CO$, 500 MHz) δ 11.59 (br s, 1h), 8.39 (d, J = 8.8 Hz, 2H), 8.25 (d, J = 8.8 Hz, 2H), 7.86 (d, J = 6.1 Hz, 2H), 7.62 (d, J = 7.6 Hz, 2H), 7.39−7.48 (m, 5H), 7.26−7.30 (m, 1H); $^{13}C\{^1H\}$ NMR ($(CD_3)_2CO$, 125 MHz) δ 170.8, 168.0, 150.5, 146.5, 146.5, 139.7, 134.26, 132.3, 131.3, 130.4, 129.8, 129.2, 127.8, 127.6, 125.0, 124.3; IR ν (cm^{-1}) 1566, 1500, 1386, 1262; HRMS (NSI+) m/z $[M + H]^+$ calcd for $C_{21}H_{15}N_5O_4H$ 402.1197, found 402.1189.

*(E)-3,4-Diphenyl-8-(4-styrylphenyl)-1,6-dioxa-2,4,7,9-tetraazaspiro[4.4]nona-2,7-diene (**32**).* Compound **32** was obtained in 77% yield (77 mg) as a light-yellow solid: R_f 0.65 (5:2 Hex/EA); mp 140−141 °C (decomposed); ^{1}H NMR ($CDCl_3$, 400 MHz) δ 8.05−7.99 (m, 2H), 7.73−7.68 (m, 2H), 7.64−7.61 (m, 2H), 7.49−7.45 (m, 3H), 7.39−7.32 (m, 5H), 7.25−7.20 (m, 1H), 7.16 (br d, J = 7.4 Hz), 6.89 (d, J = 15.8 Hz, 0.70 H), 6.56 (d, J = 16.4 Hz, 0.3 H); $^{13}C\{^1H\}$ NMR ($CDCl_3$,125 MHz) δ mixture of rotamers; IR ν (cm^{-1}) 3186, 2923, 2361, 1575, 1521, 1498, 1398; HRMS (ESI+) m/z $[M + H]^+$ calcd for $C_{23}H_{18}N_5O_4$ 428.1353, found 428.1361.

*3,4,6,8-Tetraphenyl-1-oxa-2,4,6,7,9-pentaazaspiro[4.4]nona-2,7-diene (**33**).* Compound **33** was obtained in 72% yield (73 mg) as a yellow-orange solid: R_f 0.59 (5:2 Hex/EA); mp 95−97 °C (decomposed); ^{1}H NMR ($(CD_3)_2CO$, 500 MHz) δ 10.76 (br s, 1H), 8.10 (d, J = 6.7 Hz, 2H), 7.73 (d, J = 7.5 Hz, 2H), 7.57 (d, J = 6.8 Hz, 2H), 7.41−7.47 (m, 3H), 7.19−7.32 (m, 6H), 7.03−7.11 (m, 2H), 6.81−6.95 (m, 3H); $^{13}C\{^1H\}$ NMR ($(CD_3)_2CO$, 125 MHz) δ 160.7, 153.1, 148.4, 142.6, 138.6, 133.8, 132.4, 130.3, 130.3, 130.1, 129.8, 129.5, 129.4, 129.2, 129.0, 128.6, 126.9, 124.9, 124.7, 122.5; IR ν (cm^{-1}) 1498, 1438, 1282; HRMS (NSI+) m/z $[M + H]^+$ calcd for $C_{27}H_{21}N_5OH$ 432.1819, found 432.1811.

*3-(4-Methoxyphenyl)-4,6,8-triphenyl-1-oxa-2,4,6,7,9-pentaazaspiro[4.4]nona-2,7-diene (**34**).* Compound **34** was obtained in 75% yield (76 mg) as a yellow solid: R_f 0.48 (5:2 Hex/EA); mp 117−118 °C (decomposed); ^{1}H NMR ($(CD_3)_2CO$, 400 MHz) δ 10.55 (br s, 1H), 8.10 (d, J = 8.0 Hz, 2H), 7.72 (d, J = 7.1 Hz, 2H), 7.49 (d, J = 9.0 Hz, 2H), 7.41−7.45 (m, 3H), 7.29 (t, J = 7.3 Hz, 2H), 7.19−7.23 (m, 1H), 7.06−7.10 (m, 2H), 6.84−6.90 (m, 3H), 6.79−6.81 (d, J = 8.9 Hz, 2H), 3.74 (s, 3H); $^{13}C\{^1H\}$ NMR ($(CD_3)_2CO$, 100 MHz) δ 162.7, 161.7, 154.2, 149.2, 143.8, 139.6, 133.4, 131.6, 131.1, 130.7, 130.4, 129.61, 127.9, 126.9, 125.9, 125.6, 123.5, 115.5, 56.6; IR ν (cm^{-1}) 2918, 1502, 1446, 1260, HRMS (ESI+) m/z $[M + H]^+$ calcd for $C_{28}H_{23}N_5O_2H$ 462.1925, found 462.1923.

*3-(4-Fluorophenyl)-4,6,8-triphenyl-1-oxa-2,4,6,7,9-pentaazaspiro[4.4]nona-2,7-diene (**35**).* Compound **35** was obtained in 67% yield (66 mg) as a white solid: R_f 0.63 (5:2 Hex/EA); mp 115−118 °C (decomposed); ^{1}H NMR ($(CD_3)_2CO$, 500 MHz) δ 10.81 (br s, 1H), 8.09 (d, J = 6.9 Hz, 2H), 7.72 (d, J = 7.6 Hz, 2H), 7.60 (dd, J = 8.1, 5.5 Hz, 2H), 7.42−7.47 (m, 3H), 7.30 (t, J = 7.5 Hz, 2H), 7.23 (d, J = 7.2 Hz, 1H), 7.09 (t, J = 7.7 Hz, 2H), 7.04 (t, J = 8.7 Hz, 2H), 6.85−6.92 (m, 3H); $^{13}C\{^1H\}$ NMR ($(CD_3)_2CO$, 125 MHz) δ 164.2 (J = 247.9 Hz), 160.8, 152.9, 147.6, 142.5, 138.5, 132.3, 131.35 (J = 8.2 Hz), 130.1, 129.9, 129.5, 129.4, 128.7, 126.9, 125.0, 124.9, 122.6, 115.95 (J = 21.8 Hz); IR ν (cm^{-1}) 2958, 1508, 1230; HRMS (NSI+) m/z $[M + H]^+$ calcd for $C_{27}H_{20}N_5OFH$ 450.1725, found 450.1721.

*4,6,8-Triphenyl-3-(4-(trifluoromethyl)phenyl)-1-oxa-2,4,6,7,9-pentaazaspiro[4.4]nona-2,7-diene (**36**).* Compound **36** was obtained in 69% yield (76 mg) as yellow-brown solid: R_f 0.69 (5:2 Hex/EA); mp 125−127 °C (decomposed); ^{1}H NMR ($(CD_3)_2CO$, 500 MHz) δ 11.15 (br s, 1H), 8.10 (d, J = 6.6 Hz, 2H), 7.80 (d, J = 7.9 Hz, 2H), 7.74 (m, J = 7.5 Hz, 2H), 7.64 (m, J = 7.9 Hz, 2H), 7.64 (m, J = 7.9 Hz, 2H), 7.42−7.47 (m, 3H), 7.30 (t, J = 7.6 Hz, 2H), 7.22 (t, J = 7.3 Hz, 1H), 7.07−7.12 (m, 2H), 6.85−6.93 (m, 3H); $^{13}C\{^1H\}$ NMR ($(CD_3)_2CO$, 125 MHz) δ 160.8, 152.8, 147.5, 142.2, 138.5, 137.9, 132.3, 131.5, 131.2, 130.2, 130.0, 129.7, 129.6, 129.5, 128.79, 126.9, 126.01−126.08 (q, J = 4.5 Hz), 125.07, 125.02, 122.5; IR ν (cm^{-1}) 2974, 1508, 1322, 1118, 1052; HRMS (NSI+) m/z $[M + H]^+$ calcd for $C_{28}H_{20}N_5OF_3H$ 500.1693, found 500.1683.

*3-(4-Nitrophenyl)-4,6,8-triphenyl-1-oxa-2,4,6,7,9-pentaazaspiro-[4.4]nona-2,7-diene (**37**).* Compound **37** was obtained in 61% yield (64 mg) as a light-yellow solid: R_f 0.57 (5:2 Hex/EA); mp 130−132 °C (decomposed); ^{1}H NMR ($(CD_3)_2CO$, 500 MHz) δ 11.32 (br s, 1H), 8.15 (d, J = 8.8 Hz, 2H), 8.09 (d, J = 6.6 Hz, 2H), 7.84 (d, J = 8.8 Hz, 2H), 7.73 (d, J = 7.5 Hz, 2H), 7.45 (d, J = 7.5 Hz, 3H), 7.30 (t, J = 7.6 Hz, 2H), 7.23 (t, J = 7.3 Hz, 1H), 7.05−7.14 (m, 2H), 6.85−6.97 (m, 3H); $^{13}C\{^1H\}$ NMR ($(CD_3)_2CO$, 125 MHz) δ 160.9, 152.7, 149.2, 147.1, 142.0, 140.2, 138.4, 132.2, 130.2, 130.1, 129.6, 129.5, 128.9, 126.9, 125.3, 125.1, 124.3, 122.6, 118.9; IR ν (cm^{-1}) 1698, 1498, 1334; HRMS (NSI+) m/z $[M + H]^+$ calcd for $C_{27}H_{20}N_6O_3H$ 477.1670, found: 477.1661.

In Vitro Assay against Plasmodium falciparum. Plasmodium falciparum In Vitro Culture. *Plasmodium falciparum* 3D7 wild-type parasites were cultured *in vitro* as previously described[45] using human erythrocytes kindly donated by the Australian Red Cross Blood Bank (human ethics approval HEC17−013). Briefly, *P. falciparum* cells were cultured in complete RPMI media at 4% hematocrit, 37 °C, and under low oxygen conditions (1% O_2, 5% CO_2, 94% N_2). The parasite load (or parasitemia) was assessed by light microscopy at a 1000× oil immersion magnification of Giemsa-stained thin blood smears.

Phenotypic Assays. Synchronized ring-stage parasites were purified using a well-established sorbitol method:[46] 10 μM of the spirocyclic compound was added to a 2% ring-stage *P. falciparum* culture, and parasitemia was monitored daily by blood smears over a period of 72 h. The total parasite load was determined by microscopy and parasite morphology compared to the no drug (DMSO alone) control.

Parasite Growth Assays (IC_{50}). Asynchronous parasite cultures (i.e., a mixture of ring, trophozoite, and schizont stages) at 0.25% parasitemia in 2% hematocrit were incubated with increasing concentrations of compound (up to 50 μM) in standard culture conditions. Each drug concentration was tested in triplicate.

https://dx.doi.org/10.1021/acs.joc.0c02424
J. Org. Chem. XXXX, XXX, XXX−XXX

Following 72 h of drug incubation (i.e., 2 full parasite erythrocytic cycles), cultures were subjected to a freeze/thaw cycle (to release parasite DNA material) and incubated with the DNA intercalant SYBR Gold following manufacturer instructions (SYBR Gold Nucleic Acid Stain, Invitrogen). Fluorescence was measured at 495 nm in a CLARIOstar microplate reader and analyzed as a proxy of parasite survival. The percentage of growth inhibition was plotted against the logarithm of drug concentration using GraphPad Prism v8. The resulting nonlinear regression curve determines the compound concentration (μM) that inhibits the growth of 50% of the parasite population (IC_{50}); 50 μM artemisinin and chloroquine were used as a positive inhibition control, and DMSO was used as a negative control. For each compound in this study, a minimum of four independent biological replicates was performed. The data for all assays are expressed as the mean ± standard deviation (SD) of a minimum of three independent biological replicates, each performed in triplicate.

■ ASSOCIATED CONTENT

Supporting Information

The Supporting Information is available free of charge at https://pubs.acs.org/doi/10.1021/acs.joc.0c02424.

Spectra of new compounds, including ^{1}H and ^{13}C NMR; optimization tables, biological data for compounds **26**, **36**, and **37**; crystal data (PDF)

Accession Codes

CCDC 2034794 contains the supplementary crystallographic data for this paper. These data can be obtained free of charge via www.ccdc.cam.ac.uk/data_request/cif, or by emailing data_request@ccdc.cam.ac.uk, or by contacting The Cambridge Crystallographic Data Centre, 12 Union Road, Cambridge CB2 1EZ, UK; fax: +44 1223 336033.

■ AUTHOR INFORMATION

Corresponding Author

Pallavi Sharma − *La Trobe Institute for Molecular Science, La Trobe University, Melbourne, Victoria 3086, Australia; School of Chemistry, Joseph Bank Laboratory, University of Lincoln, Lincoln LN6 7TS, United Kingdom;* orcid.org/0000-0001-5226-7864; Email: p.sharma@latrobe.edu.au

Authors

M. R. Ranga Prabhath − *School of Chemistry, Joseph Bank Laboratory, University of Lincoln, Lincoln LN6 7TS, United Kingdom*

Derek Wong − *Department of Physiology, Anatomy and Microbiology, La Trobe University, Melbourne, Victoria 3086, Australia*

Maame Adjoa Ampem-Lassen − *La Trobe Institute for Molecular Science, La Trobe University, Melbourne, Victoria 3086, Australia*

Shreesha V. Bhat − *School of Chemistry, Joseph Bank Laboratory, University of Lincoln, Lincoln LN6 7TS, United Kingdom*

Luke Williams − *School of Chemistry, Joseph Bank Laboratory, University of Lincoln, Lincoln LN6 7TS, United Kingdom*

Teresa G. Carvalho − *Department of Physiology, Anatomy and Microbiology, La Trobe University, Melbourne, Victoria 3086, Australia;* orcid.org/0000-0002-4947-371X

Complete contact information is available at: https://pubs.acs.org/10.1021/acs.joc.0c02424

Notes

The authors declare no competing financial interest.

■ ACKNOWLEDGMENTS

P.S. would like to thank the EPSRC (EP/N00969X/1) for research funding (M.R.R.P.). We thank the University of Lincoln for Ph.D. studentship funding (S.V.B. and L.W.). We thank the National Mass Spectrometry Facility at Swansea University and the Australian Red Cross Lifeblood for providing human erythrocytes (human ethics HEC17-013). We thank Ms. Coralie Boulet (LTU) for performing parasite growth assays with artemisinin and chloroquine and Dr. Elisa Nauha (UoL) and Jie Sun (Shanghai Institute of Organic Chemistry, China) for X-ray crystallography.

■ REFERENCES

(1) Müller, G.; Berkenbosch, T.; Benningshof, J. C. J.; Stumpfe, D.; Bajorath, J. Charting biologically relevant spirocyclic compound space. *Chem. - Eur. J.* **2017**, *23*, 703−710.

(2) Zheng, Y. J.; Tice, C. M. The utilization of spirocyclic scaffolds in novel drug discovery. *Expert Opin. Drug Discovery* **2016**, *11*, 831−834.

(3) Carreira, E. M.; Fessard, T. C. Four-membered ring-containing spirocycles: Synthetic strategies and opportunities. *Chem. Rev.* **2014**, *114*, 8257−8322.

(4) Kidd, S. L.; Osberger, T. J.; Mateu, N.; Sore, H. F.; Spring, D. R. Recent applications of diversity-oriented synthesis toward novel, 3-dimensional fragment collections. *Front. Chem.* **2018**, *6*, 460.

(5) Kim, S.; Ko, H.; Lee, T.; Kim, D. Formal Synthesis of (−)-Perhydrohistrionicotoxin via Cyclic Amino Acid Ester-Enolate Claisen Rearrangement and Ring-Closing Metathesis. *J. Org. Chem.* **2005**, *70*, 5756−5759.

(6) Oxford, A. E.; Raistrick, H.; Simonart, P. Studies in the biochemistry of micro-organisms: Griseofulvin, C17H17O6Cl, a metabolic product of Penicillium griseo-fulvum Dierckx. *Biochem. J.* **1939**, *33*, 240−248.

(7) Taylor, F. F.; Faloon, W. W. The Role of potassium in the natriuretic response to a steroidal lactone (SC-9420). *J. Clin. Endocrinol. Metab.* **1959**, *19*, 1683−1687.

(8) Brunner, H. R. The new angiotensin II receptor antagonist, Irbesartan: Pharmacokinetic and pharmacodynamic considerations. *Am. J. Hypertens.* **1997**, *10*, 311S−317S.

(9) Lovering, F.; Bikker, J.; Humblet, C. Escape from flatland: Increasing saturation as an approach to improving clinical success. *J. Med. Chem.* **2009**, *52*, 6752−6756.

(10) Wermuth, C. G.; Villoutreix, B.; Grisoni, S.; Olivier, A.; Rocher, J. P. In *The Practice of Medicinal Chemistry*; Wermuth, C., Aldous, D., Raboisson, P., Rognan, D., Eds.; Academic Press: London, 2015; pp 73−96.

(11) Kotha, S.; Chandra Deb, A.; Lahiri, K.; Manivannan, E. Selected synthetic strategies to spirocyclics. *Synthesis* **2009**, *2*, 165−193.

(12) Huisgen, R. 1,3-Dipolar Cycloadditions. Past and future. *Angew. Chem., Int. Ed. Engl.* **1963**, *2*, 565−598.

(13) Huisgen, R. Kinetics and mechanism of 1,3-dipolar cycloadditions. *Angew. Chem., Int. Ed. Engl.* **1963**, *2*, 633−645.

(14) Day, J.; Uroos, M.; Castledine, R. A.; Lewis, W.; McKeever-Abbas, B.; Dowden, J. Alkaloid inspired spirocyclic oxindoles from 1,3-dipolar cycloaddition of pyridinium ylides. *Org. Biomol. Chem.* **2013**, *11*, 6502.

(15) Wu, L.; Sun, J.; Yan, C.-G. Facile synthesis of spiro[indoline-3,3′-pyrrolo[1,2-a]quinolines] and spiro[indoline-3,1′-pyrrolo[2,1-a]-isoquinolines] via 1,3-dipolar cycloaddition reactions of heteroaromatic ammonium salts with 3-phenacylideneoxindoles. *Org. Biomol. Chem.* **2012**, *10*, 9452−9463.

(16) Liu, H.; Jia, H.; Wang, B.; Xiao, Y.; Guo, H. Synthesis of spirobidihydropyrazole through double 1,3-dipolar cycloaddition of nitrilimines with allenoates. *Org. Lett.* **2017**, *19*, 4714−4717.

(17) Wang, D.; Wei, Y.; Shi, M. Construction of adjacent spiro-quaternary and tertiary stereocenters through phosphine-catalyzed

asymmetric [3 + 2] annulation of allenoates with alkylidene azlactones. *Chem. Commun.* **2012**, *48*, 2764−2766.
(18) Huisgen, R.; Grashey, R.; Kunz, R.; Wallbillich, G.; Aufderhaar, E. 1.3-Dipolare cycloadditionen, XVII: Bisaddukte aus nitriliminen und carbodiimiden. *Chem. Ber.* **1965**, *98*, 2174−2184.
(19) Huisgen, R.; Aufderhaar, E. 1.3-Dipolare Cycloadditionen, XVIII: Die umsetzung des phenyl-cyanamids mit C-Äthoxycarbonyl-N-phenyl-nitrilimin. *Chem. Ber.* **1965**, *98*, 2185−2192.
(20) Huisgen, R.; Aufderhaar, E.; Wallbillich, G. 1.3-Dipolare Cycloadditionen, XVI: Zur bildung von 1.4-dihydro-tetrazinen aus nitriliminen; 1.4-diphenyl-1.4-dihydro-1.2.4.5-tetrazin und isomere verbindungen. *Chem. Ber.* **1965**, *98*, 1476−1486.
(21) Prabhath, M. R. R.; Williams, L.; Bhat, S. V.; Sharma, P. Recent advances in cyanamide chemistry: Synthesis and applications. *Molecules* **2017**, *22*, 615.
(22) Direct translation from German: ref 19.
(23) Bhat, S. V.; Robinson, D.; Moses, J. E.; Sharma, P. Synthesis of oxadiazol-5-imines via the cyclizative capture of in situ generated cyanamide ions and nitrile oxides. *Org. Lett.* **2016**, *18*, 1100−1103.
(24) Sharma, P.; Bhat, S. V.; Prabhath, M. R. R.; Molino, A.; Nauha, E.; Wilson, D. J. D.; Moses, J. E. Synthesis of 1,2,4-triazol-3-imines via selective stepwise cycloaddition of nitrile imines with organo-cyanamides. *Org. Lett.* **2018**, *20*, 4263−4266.
(25) Tremoli, E.; Maderna, P.; Cocuzza, E.; Mantero, O. Platelet antiaggregating activity of imolamine: In vitro studies. *Pharmacol. Res. Commun.* **1979**, *11*, 31−38.
(26) Muller, P. Glossary of terms used in physical organic chemistry. *Pure Appl. Chem.* **1994**, *66*, 1077−1184.
(27) Moss, G. P. Extension and revision of the nomenclature for spiro compounds. *Pure Appl. Chem.* **1999**, *71*, 531−558.
(28) Spiteri, C.; Sharma, P.; Zhang, F.; Macdonald, S. J. F.; Keeling, S.; Moses, J. E. An improved synthesis of 1,2-benzisoxazoles: TBAF mediated 1,3-dipolar cycloaddition of nitrile oxides and benzyne. *Chem. Commun.* **2010**, *46*, 1272−1274.
(29) Spiteri, C.; Keeling, S.; Moses, J. E. New Synthesis of 1-substituted-1H-indazoles via 1,3-dipolar cycloaddition of in situ generated nitrile imines and benzyne. *Org. Lett.* **2010**, *12*, 3368−3371.
(30) Spiteri, C.; Mason, C.; Zhang, F.; Ritson, D. J.; Sharma, P.; Keeling, S.; Moses, J. E. An efficient entry to 1,2-benzisoxazoles via 1,3-dipolar cycloaddition of in situ generated nitrile oxides and benzyne. *Org. Biomol. Chem.* **2010**, *8*, 2537−2542.
(31) Gasco, A.; Boulton, A. J. Furoxans and benzofuroxans. *Adv. Heterocycl. Chem.* **1981**, *29*, 251−340.
(32) Chiang, Y. H. Chlorination of oximes. I. Reaction and mechanism of the chlorination of oximes in commercial chloroform and methylene chloride. *J. Org. Chem.* **1971**, *36*, 2146−2155.
(33) Wiley, R. H.; Wakefield, B. J. Infrared spectra of the nitrile N-oxides: Some New Furoxans. *J. Org. Chem.* **1960**, *25*, 546−551.
(34) Murillo, F.; Barroso, J.; de los Santos, M. G.; Ávila, G.; Pan, S.; Fernandez-Herrera, M. A.; Merino, G. Revisiting the formation mechanism of 1,3,4-Oxadiazole-2(3H)-ones from hydrazonyl chloride and carbon dioxide. *J. Org. Chem.* **2018**, *83*, 13045−13050.
(35) Dubrovskiy, A. V.; Larock, R. C. Synthesis of benzisoxazoles by the [3 + 2] cycloaddition of in situ generated nitrile oxides and arynes. *Org. Lett.* **2010**, *12*, 1180−1183.
(36) CSD Deposition Number CCDC 2034794.
(37) The isolated spiranes were stable in solid form when stored at ambient conditions over several days. ^{1}H NMR spectra of **25** stored in DMSO-d_6 over 16 days showed no change in spectra (see Supporting Information).
(38) Chen, W.; Wang, B.; Liu, N.; Huang, D.; Wang, X.; Hu, Y. Tandem synthesis of 3-halo-5-substituted isoxazoles from 1-copper(I) alkynes and dihaloformaldoximes. *Org. Lett.* **2014**, *16*, 6140−6143.
(39) Dineen, T. A.; Chen, K.; Cheng, A. C.; Derakhchan, K.; Epstein, O.; Esmay, J.; Hickman, D.; Kreiman, C. E.; Marx, I. E.; Wahl, R. C.; Wen, P. H.; Weiss, M. M.; Whittington, D. A.; Wood, S., Jr.; Fremeau, R. T.; White, R. D.; Patel, V. F. Inhibitors of β-site amyloid precursor protein cleaving enzyme (BACE1): Identification of (S)-7-(2-fluoropyridin-3-yl)-3-((3-methyloxetan-3-yl)ethynyl)-5′H-spiro[chromeno[2,3-b]pyridine-5,4′-oxazol]-2′-amine (AMG-8718). *J. Med. Chem.* **2014**, *57*, 9811−9831.
(40) Basarab, G. S.; Doig, P.; Galullo, V.; Kern, G.; Kimzey, A.; Kutschke, A.; Newman, J. P.; Morningstar, M.; Mueller, J.; Otterson, L.; Vishwanathan, K.; Zhou, F.; Gowravaram, M. Discovery of novel DNA gyrase inhibiting spiropyrimidinetriones: Benzisoxazole fusion with N-linked oxazolidinone substituents leading to a clinical candidate (ETX0914). *J. Med. Chem.* **2015**, *58*, 6264−6282.
(41) *World malaria report*, 2019.
(42) Zhang, J. F. *As Detailed Chronological Record of Project 523 and the Discovery and Development of Qinghaosu (Artemisinin)*; Yang Cheng Evening News Publishing Company, 2005.
(43) van der Pluijm, R. W; Imwong, M.; Chau, N. H.; Hoa, N. T.; Thuy-Nhien, N. T.; Thanh, N. V.; Jittamala, P.; Hanboonkunupakarn, B.; Chutasmit, K.; Saelow, C.; Runjarern, R.; Kaewmok, W.; Tripura, R.; Peto, T. J; Yok, S.; Suon, S.; Sreng, S.; Mao, S.; Oun, S.; Yen, S.; Amaratunga, C.; Lek, D.; Huy, R.; Dhorda, M.; Chotivanich, K.; Ashley, E. A; Mukaka, M.; Waithira, N.; Cheah, P. Y.; Maude, R. J; Amato, R.; Pearson, R. D; Goncalves, S.; Jacob, C. G; Hamilton, W. L; Fairhurst, R. M; Tarning, J.; Winterberg, M.; Kwiatkowski, D. P; Pukrittayakamee, S.; Hien, T. T.; Day, N. P.; Miotto, O.; White, N. J; Dondorp, A. M; et al. Determinants of dihydroartemisinin-piperaquine treatment failure in Plasmodium falciparum malaria in Cambodia, Thailand, and Vietnam: a prospective clinical, pharmacological, and genetic study. *Lancet Infect. Dis.* **2019**, *19*, 952−961.
(44) Gamo, F. J.; Sanz, L. M.; Vidal, J.; de Cozar, C.; Alvarez, E.; Lavandera, J. L.; Vanderwall, D. E.; Green, D. V. S.; Kumar, V.; Hasan, S.; Brown, J. R.; Peishoff, C. E.; Cardon, L. R.; Garcia-Bustos, J. F. Thousands of chemical starting points for antimalarial lead identification. *Nature* **2010**, *465*, 305−310.
(45) Trager, W.; Jensen, J. B. Human malaria parasites in continuous culture. *Science* **1976**, *193*, 673−675.
(46) Lambros, C.; Vanderberg, J. P. Synchronization of *Plasmodium falciparum* erythrocytic stages in culture. *J. Parasitol.* **1979**, *65*, 418−420.

https://dx.doi.org/10.1021/acs.joc.0c02424
J. Org. Chem. XXXX, XXX, XXX−XXX